Gravitational Radiation from Coalescing Supermassive Black Hole Binaries in a Hierarchical Galaxy Formation Model

Motohiro Enoki * [1], Kaiki T. Inoue[2], Masahiro Nagashima[3] and Naoshi Sugiyama[1]
[1]National Astronomical Observatory of Japan, Tokyo 181-8588, Japan
[2]Department of Natural Science and Engineering, Kinki University, Higashi-Osaka, Osaka, 577-8502, Japan and
[3]Department of Physics, Kyoto University, Sakyo-ku, Kyoto, 606-8502, Japan

We investigate the expected gravitational wave emission from coalescing supermassive black hole (SMBH) binaries resulting from mergers of their host galaxies. We employ a semi-analytic model of galaxy and quasar formation based on the hierarchical clustering scenario to estimate the amplitude of the expected stochastic gravitational wave background owing to inspiraling SMBH binaries and bursts rates owing to the SMBH binary coalescence events. We find that the characteristic strain amplitude of the background radiation is $h_c(f) \sim 10^{-16}(f/1\mu\mathrm{Hz})^{-2/3}$ for $f \lesssim 1\mu$Hz. The main contribution to the total strain amplitude of the background radiation comes from SMBH coalescence events at $0 < z < 1$. We also find that a future space-based gravitational wave interferometer such as the planned *Laser Interferometer Space Antenna* (*LISA*) might detect intense gravitational wave bursts associated with coalescence of SMBH binaries with total mass $M_{\rm tot} < 10^7 M_\odot$ at $z \gtrsim 2$ at a rate ~ 1.0 yr^{-1}. Our model predicts that burst signals with a larger amplitude $h_{\rm burst} \sim 10^{-15}$ correspond to coalescence events of massive SMBH binary with total mass $M_{\rm tot} \sim 10^8 M_\odot$ at low redshift $z \lesssim 1$ at a rate ~ 0.1 yr^{-1} whereas those with a smaller amplitude $h_{\rm burst} \sim 10^{-17}$ correspond to coalescence events of less massive SMBH binary with total mass $M_{\rm tot} \sim 10^6 M_\odot$ at high redshift $z \gtrsim 3$.

1. INTRODUCTION

In recent years, there has been increasing observational evidence that many nearby galaxies have central supermassive black holes (SMBHs) in the mass range of $10^6 - 10^9 M_\odot$, and that their physical properties correlate with those of spheroids of their host galaxies. This suggests that the formation of SMBHs physically links to the formation of spheroids that harbor the SMBHs. Therefore, in order to study the formation and evolution of SMBHs, it is necessary to construct a model that includes galaxy formation processes.

In the standard hierarchical structure formation scenario in a cold dark matter (CDM) universe, dark-matter halos (*dark halos*) cluster gravitationally and merge together. In each of merged dark halos, a galaxy is formed as a result of radiative gas cooling, star formation, and supernova feedback. Several galaxies in a common dark halo sometimes merge together and a more massive galaxy is assembled. When galaxies merge, SMBHs in the centers of the galaxies sink toward the center of the new merged galaxy and form a SMBH binary subsequently. If the binary loses enough energy and angular momentum, it will evolve to the gravitational wave emitting regime and begin inspiraling, eventually coalesces with a gravitational wave burst.

An ensemble of gravitational waves from a number of inspiraling SMBH binaries at different redshift can be observed as a stochastic background at frequencies $\sim 1\mathrm{n} - 1\mu$Hz, which can be detected by pulsar timing measurements. Future space interferometers such as the *Laser Interferometer Space Antenna* (*LISA*) might detect quasi-monochromatic wave sources associated with inspiraling SMBH binaries and gravitational wave bursts associated with SMBH binary coalescence [e.g. 1].

To date, a number of attempts have been made to calculate the SMBH coalescence rate. Some authors use phenomenological models of galaxy mergers based on number counts of quasars and spheroids [e.g. 2, 3]. Others use merger rates of dark halos (not galaxies) [e.g. 1]. However, none of these models include baryonic gas evolution and galaxy formation processes. Because SMBH formation process is relevant to spheroids of host galaxies rather than to dark halos, we need to evaluate how the baryonic gas processes such as star formation and supernova feedback affect the SMBH formation process.

In this study, we estimate the SMBH coalescence rate using a new semi-analytic (SA) model [4] (an extended model [5]) in which the SMBH formation is incorporated into the galaxy formation. Then, we calculate the spectrum of gravitational wave background from inspiraling SMBH binaries, based on the formulation given by Jaffe & Backer [2] and we compare our result with that from a pulsar timing measurement. We also estimate the event rate of gravitational wave bursts from SMBH coalescence events that might be detected by future planned space laser interferometers, based on an argument in [3]. The details of formulation, results, discussion and references are given in [6].

*enoki.motohiro@nao.ac.jp

2. GALAXY MERGER / BLACK HOLE COALESCENCE RATE

Here we briefly describe our SA model for galaxy formation and SMBH growth. The details are shown in [5] and [4].

2.1. The model of galaxy formation

First, we construct Monte Carlo realizations of merging histories of dark halos from the present to higher redshifts. Merging histories of dark halos depend on the cosmological model. The adopted cosmological model is a low-density, spatially flat cold dark matter (ΛCDM) universe with the present density parameter, $\Omega_{\rm m} = 0.3$, the cosmological constant, $\Omega_\Lambda = 0.7$, the Hubble constant $h = 0.7$ ($h \equiv H_0/100$ km s^{-1} Mpc^{-1}) and the present rms density fluctuation in spheres of $8h^{-1}$Mpc radius, $\sigma_8 = 0.9$. The highest redshift in each merging path which depends on the present dark halo mass, is about $z \sim 20 - 30$.

Next, in each merging path of dark halos, we calculate the evolution of the baryonic component from higher redshifts to the present using simple analytic models for gas cooling, star formation, supernova feedback, galaxy merging and other processes. When a dark halo collapses, the gas in the halo is shock-heated to the virial temperature of the halo (the *hot gas*). At the same time, the gas in dense regions of the halo cools owing to efficient radiative cooling and sinks to the center of the halo and settle into a rotationally supported disk until the subsequent collapse of the dark halo. We call this cooled gas the *cold gas*. Stars are formed from the cold gas. With star formation, supernovae occur and heat up the surrounding cold gas to the hot gas phase (supernova feedback).

When several progenitor halos have merged, a newly formed larger dark halo contains at least two or more galaxies which had originally resided in the individual progenitor halos. We identify the central galaxy in the new common halo with the central galaxy contained in the most massive of the progenitor halos. Other galaxies are regarded as *satellite galaxies*. After each merging of halo, these satellites merge by either dynamical friction or random collision. Satellite galaxies merge with the central galaxy in the dynamical friction timescale [7]. Satellite galaxies sometimes merge with each other in the timescale of random collisions. Under the condition that the satellite galaxies gravitationally bound and merge during encounters, this timescale is derived by Makino & Hut [8]. If the mass ratio, $f = m_1/m_2$, is larger than a certain critical value of $f_{\rm bulge}$, we assume that a starburst occurs, and that all of the cold gas turns into stars and hot gas, which fills the dark halo, and all of the stars populate the bulge of a new galaxy. On the other hand, if $f < f_{\rm bulge}$, no starburst occurs and a smaller galaxy is simply absorbed into the disk of a larger galaxy.

Model parameters are determined by a comparison with observations of galaxies in the local Universe, such as luminosity functions and the cold gas mass fraction in spiral galaxies. Our SA model can reproduce galaxy number counts and photometric redshift distribution of galaxies in the Hubble Deep Field [5].

2.2. The growth of SMBHs

In our model, it is assumed that SMBHs grow by coalescence when their host galaxies merge and are fueled by accreted cold gas during major mergers of galaxies. When the host galaxies merge, pre-existing SMBHs sink to the center of the new merged galaxy due to dynamical friction (or other mechanisms such as gas dynamics), evolve to the gravitational wave emission regime and eventually coalesce. Although the timescale for this process is unknown, for the sake of simplicity we assume that SMBHs instantaneously evolve to the gravitational wave emission regime and coalesce. Gas-dynamical simulations have demonstrated that the major merger of galaxies can drive substantial gaseous inflows and trigger starburst activity. Thus, it is reasonable to assume that during a major merger of galaxies, a certain fraction of the cold gas that is proportional to the total mass of stars newly formed at starburst accretes onto the newly formed SMBH and this accretion process leads to a quasar activity. Under this assumption, the mass of cold gas accreted on a SMBH is given by

$$M_{\rm acc} \;=\; f_{\rm BH} \Delta M_{*,\rm burst}, \qquad (1)$$

where $f_{\rm BH}$ is a constant and $\Delta M_{*,\rm burst}$ is the total mass of stars formed at starburst. The free parameter of $f_{\rm BH}$ is fixed by matching the observed relation between a spheroid mass and a black hole mass $M_{\rm BH}/M_{\rm spheroid} = 0.001 - 0.006$ (e.g. [9]); we find that the favorable value of $f_{\rm BH}$ is nearly 0.03.

Figure 1 (a) shows the black hole mass functions in our model at a series of various redshifts. In this figure, we superpose the observed black hole mass function at $z = 0$ [10]. The predicted mass function is quite consistent with the observation. Our galaxy formation model includes dynamical friction and random collision as galaxy merging mechanisms. For comparison, in figure 1 (b), we also plot the black hole mass functions at $z = 0$ of other two models: no random collision model (no rc model) and no dynamical friction model (no df model). In the no rc model and the no df model, mergers owing to random collision and dynamical friction, respectively, are switched off. This figure shows that the mass function for low mass black holes are determined by random collisions between satellite galaxies and that for high mass black holes

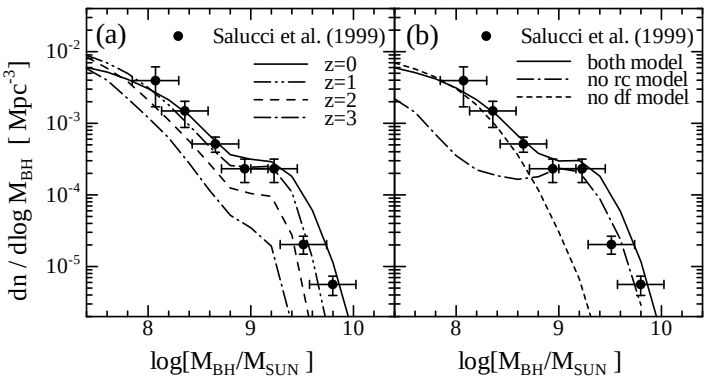

Figure 1: (a) Black hole mass function of the model at a series of redshifts. The symbols with errorbars are the observed black hole mass function at $z = 0$ [10]. (b) Black hole mass function at $z = 0$ for different galaxy merger models, which are both model, no random collision model (no rc model) and no dynamical friction model (no df model). Both model includes dynamical friction and random collision as the galaxy merging mechanism.

are influenced by dynamical friction. The shape of black hole mass function depends on detailed gas processes. The important contribution of mass increment of SMBHs in central galaxies is the cold gas, which is accreted to only central galaxies. SNe feedback removes this cold gas more efficiently in smaller galaxies with $V_{\rm circ} < 280{\rm km\ s^{-1}}$ ($M_{\rm gal} < 10^{12} M_\odot$). Thus, the growth of the SMBHs in small galaxies suffers from SNe feedback. In the no rc model, SMBHs mainly exist central galaxies. Therefore, the shape of the black hole mass function in the no rc model has a bump at high mass end ($M_{\rm BH} \sim 10^9 M_\odot$) which corresponds to SMBHs in the central galaxies ($M_{\rm gal} \sim 10^{12} M_\odot$). On the other hand, in the no df model, high mass SMBHs cannot be produced since galaxies cannot merge with the massive central galaxy.

Using the SA model incorporated with this SMBH growth model, we estimate the comoving number density, $n_c(M_1, M_2, z) dM_1 dM_2 dz$, of the coalescing SMBH binaries with mass $M_1 \sim M_1 + dM_1$ and $M_2 \sim M_2 + dM_2$ at z in a given redshift interval dz.

3. GRAVITATIONAL RADIATION

3.1. Background radiation from SMBH binaries

In order to calculate the spectrum of gravitational wave background radiation from SMBH binaries, we improve the formulation of Jaffe & Backer [2]. The details are described in [6]. The spectrum of the gravitational wave background radiation which we finally obtain is

$$h_c^2(f) = \int dz\, dM_1\, dM_2\, \frac{4\pi c^3}{3} \left(\frac{G M_{\rm chirp}}{c^3}\right)^{5/3} (\pi f)^{-4/3} \times (1+z)^{-1/3} n_c(M_1, M_2, z)\, \theta(f_{\rm max} - f), \quad (2)$$

where $M_{\rm chirp} = [M_1 M_2 (M_1 + M_2)^{-1/3}]^{3/5}$ is the chirp mass of the system and c is the speed of light, f is the observed frequency of the gravitational wave from the binary in a circular orbit, the $f_{\rm max}$ is maximum frequency and $\theta(x)$ is the step function. As a SMBH binary evolves with time, the frequency becomes higher. We assume that the binary orbit is quasi-stationary until the radius equals to $3R_{\rm S}$, where $R_{\rm S}$ is the Schwarzschild radius : the radius of the innermost stable circular orbit (ISCO) for a particle and a non-rotating black hole. Then $f_{\rm max}$ is

$$\begin{aligned} f_{\rm max}(M_1, M_2, z) &= \frac{c^3}{6^{3/2}\pi G M_1 (1+z)} \left(1 + \frac{M_2}{M_1}\right)^{1/2} \\ &= 4.4 \times 10^{-5} (1+z)^{-1} \left(\frac{M_1}{10^8 M_\odot}\right)^{-1} \\ &\quad \times \left(1 + \frac{M_2}{M_1}\right)^{1/2} {\rm Hz}, \end{aligned} \quad (3)$$

where M_1 and M_2 are SMBH masses ($M_1 > M_2$).

As shown in figure 2, the spectrum changes its slope at $f \sim 1\mu$Hz owing to lack of power associated with the upper limit frequency, $f_{\rm max}$. This feature is consistent with the results of Sesana et al. [11]. The predicted strain spectrum is $h_{\rm c}(f) \sim 10^{-16} (f/1\mu{\rm Hz})^{-2/3}$ for $f \lesssim 1\mu$Hz, just below the current limit from the pulsar timing measurements [12]. In our model, we assume that SMBHs coalesce simultaneously when their host galaxies merge. Therefore, the efficiency of SMBH coalescence is maximum and the predicted amplitude of gravitational wave spectrum should be interpreted as the upper limit.

In figure 2 (a), we plot the spectra from binaries in different redshift intervals. This figure shows that the total spectrum of background radiation comes from coalescing SMBH binaries at low redshift, $0 \le z < 1$. Although the coalescence rate at low redshift is lower than at high redshift, the main contribution to the

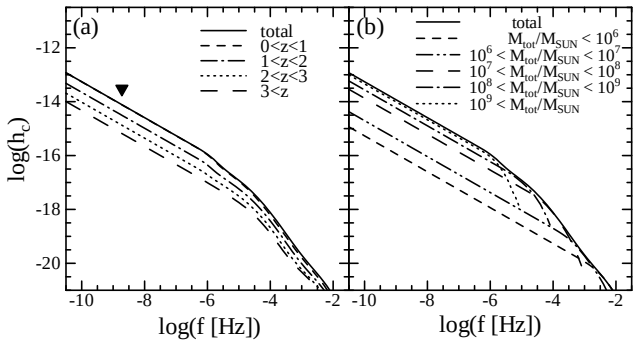

Figure 2: Spectrum of gravitational wave background radiation, $h_{\rm c}(f)$, from SMBH binaries in different redshift intervals (a) and in different total mass intervals (b). The filled reverse triangle in (a) shows the current limit from pulsar timing measurements [12].

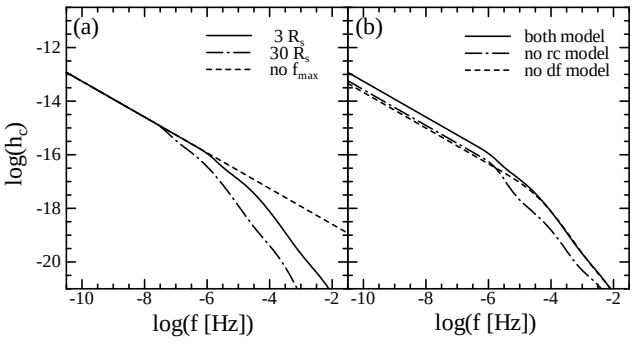

Figure 3: Spectrum of gravitational wave background radiation, $h_{\rm c}(f)$, in different $f_{\rm max}$ (a) and in different galaxy merger models (b).

background radiation is the coalescing SMBH binaries at low redshift, $0 \leq z < 1$. This is because the distance from an observer to the SMBH binaries at low redshift is shorter and the mass of SMBHs at low redshift is higher. In figure 2(b), we also plot the spectra from binaries in different total mass intervals ($M_{\rm tot} = M_1 + M_2$). This figure shows that for $f \gtrsim 10^{-4}$Hz the total spectrum of background radiation comes from coalescing SMBH binaries with total mass $M_{\rm tot} \lesssim 10^8 M_\odot$.

When SMBHs are spinning and/or when their masses are comparable, the definition of ISCO becomes vague and our assumption that the cutoff frequency $f_{\rm max}$ corresponds to $3R_{\rm S}$ may not be correct. To see the effects of the cutoff frequency, we plot the spectra for different values of $f_{\rm max}$, corresponding to $3R_{\rm S}$, $30R_{\rm S}$, and no frequency cut off, respectively (fig. 3 (a)). Lowering $f_{\rm max}$ causes a suppression in the stochastic background at high frequencies $f \lesssim 10^{-7}$Hz since a large portion of high frequency modes are cut off.

Our galaxy formation model incorporates dynamical friction and random collision as galaxy merging mechanisms. In order to examine the effect of these two galaxy merger mechanisms on the spectrum of gravitational wave background radiation, in figure 3 (b), we also plot the spectrum of background radiation of other two models: no rc model and no df model. The no df model can not produce higher mass SMBH (see fig. 1(b)). Consequently, the spectrum in no df model bends at larger frequency since the number of SMBHs with smaller $f_{\rm max}$ decreases. Furthermore, in the no df model, the amplitude of gravitational waves from each binary becomes smaller . However, the coalescence rate in no df model is higher than the rate in no rc model. As a result, the amplitude of the spectrum in no df model is roughly equal to the amplitude in no rc model.

3.2. Gravitational wave bursts from SMBH coalescence

After an inspiraling phase, SMBHs plunge into a final death inspiral and merge to form a single black hole. We call a set of a plunge and a subsequent early non-linear ring-down phase as a *burst*. We estimate the expected burst event rate per observers' time using the amplitude of burst gravitational wave given in [3], and the SMBH coalescence rate calculated by our SA model, $n_c(M_1, M_2, z)$.

The characteristic amplitude of the burst gravitational wave which we finally obtain is

$$h_{\rm burst} = \frac{3^{3/4}\epsilon^{1/2} G M_{\rm tot}}{2^{1/2}\pi c^2 D(z)} = 7.8\times10^{-16}\left(\frac{\epsilon}{0.1}\right)^{1/2}\left(\frac{M_{\rm tot}}{10^8\ M_\odot}\right)\left[\frac{D(z)}{1\ {\rm Gpc}}\right]^{-1} \quad (4)$$

where ϵ is the efficiency of the energy release, $D(z)$ is the comoving distance to the source from the observer and $f_{\rm c}$ is the observed characteristic frequency. $f_{\rm c}$ from the gravitational wave burst occurring at z is

$$f_{\rm c} = \frac{c^3}{3^{3/2} G M_{\rm tot}\ (1+z)} = 3.9\times10^{-4}\left(\frac{M_{\rm tot}}{10^8\ M_\odot}\right)^{-1}(1+z)^{-1}{\rm Hz}. \quad (5)$$

Then, we obtain $n_{\rm burst}(h_{\rm burst}, f_{\rm c}, z)\ dh_{\rm burst}\ df_{\rm c}\ dz$, which is the comoving number density of gravitational wave burst events occurring at z in a given redshift interval dz with amplitude $h_{\rm burst} \sim h_{\rm burst} + dh_{\rm burst}$ and with characteristic frequency $f_{\rm c} \sim f_{\rm c} + df_{\rm c}$. Therefore, the expected event rates of gravitational wave bursts per observers' time with amplitude $h_{\rm burst} \sim h_{\rm burst} + dh_{\rm burst}$ and characteristic frequency $f_{\rm c} \sim f_{\rm c} + df_{\rm c}$, $\nu_{\rm burst}(h_{\rm burst}, f_{\rm c})\ dh_{\rm burst}\ df_{\rm c}$ is given by

$$\nu_{\rm burst}(h_{\rm burst}, f_{\rm c}) = \int n_{\rm burst}(h_{\rm burst}, f_{\rm c}, z)\frac{dV}{dt_0}dz, \quad (6)$$

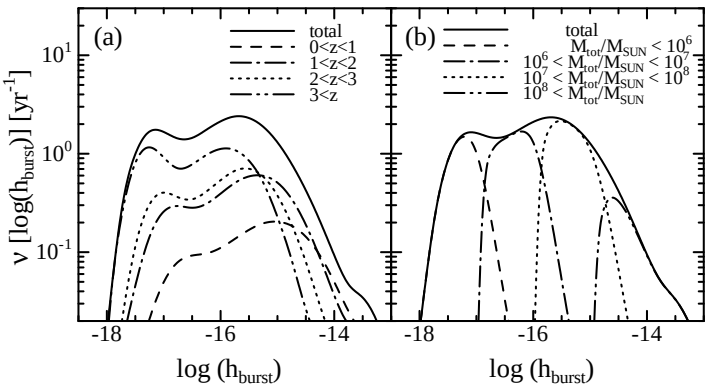

Figure 4: Integrated event rate of gravitational wave bursts from SMBH coalescence per observers' time unit a year, $\nu_{\rm burst}[\log(h_{\rm burst})]$, in different redshifts (a) and in different total mass ranges (b).

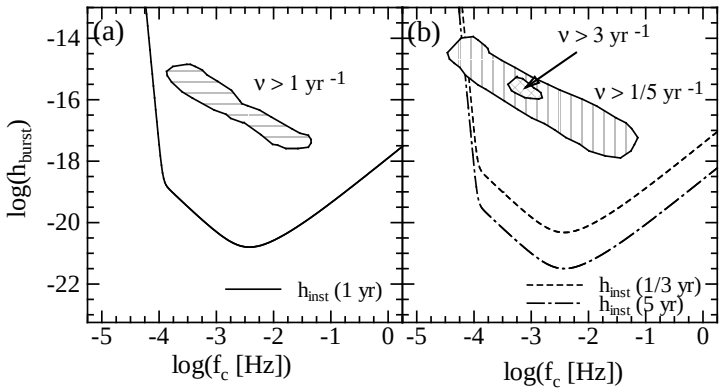

Figure 5: Expected signals of gravitational wave bursts from SMBH coalescence. (a) The horizontally hatched area shows the region, $\nu_{\rm burst}[\log(h_{\rm burst}), \log(f_{\rm c})] > 1{\rm yr}^{-1}$. The solid curve indicates the instrumental noise threshold for one year of *LISA* observations. (b) The vertically hatched area shows the region, $\nu_{\rm burst} > 1/5{\rm yr}^{-1}$ and the diagnal cross-hatched area show the region, $\nu_{\rm burst} > 3{\rm yr}^{-1}$. The dot-dashed and the short dashed lines indicates the instrumental noise threshold for 5 year and 1/3 year of *LISA* observations, respectively.

where t_0 is the observers' time and dV is the comoving volume element at z. The integrated event rates of gravitational wave bursts per observers' time with amplitude $h_{\rm burst} \sim h_{\rm burst} + dh_{\rm burst}$, $\nu_{\rm burst}(h_{\rm burst})\, dh_{\rm burst}$, are given respectively as follows,

$$\nu_{\rm burst}(h_{\rm burst}) = \int \nu_{\rm burst}(h_{\rm burst}, f_{\rm c}) df_{\rm c}. \qquad (7)$$

In figure 4, we plot the total integrated event rates of gravitational wave bursts and integrated event rates in different redshift intervals (fig. 4(a)) and in different total mass intervals in (fig. 4(b)). Here we set the efficiency of the energy release $\epsilon = 0.1$, while the precise value of this parameter is unknown. In most typical events, a conversion efficiency will probably be a few percent. From equation (4), one can see that the change of efficiency results in the parallel displacement in the horizontal direction in figure 4. The shape of $\nu_{\rm burst}(h_{\rm burst})$ reflects the black hole mass functions and the SMBH coalescence rates, which depend on the complex galaxy formation processes. In figure 4 (a), one can notice that there are two peaks in the event rate in terms of $h_{\rm burst}$. A peak at $h_{\rm burst} \sim 10^{-17}$ corresponds to bursts from SMBH binaries with $M_{\rm tot} < 10^6 M_\odot$ whose total number is the largest at high redshift $z > 3$. Another peak at $h_{\rm burst} \sim 10^{-15}$ corresponds to bursts from SMBH binaries with $10^7 M_\odot < M_{\rm tot} < 10^8 M_\odot$ whose coalescence probability is the largest at low redshift $z < 3$. Figure 4 (b) indicates that burst signals with large amplitude ($h_{\rm burst} \gtrsim 10^{-15}$) correspond to coalescence of "massive" SMBH binaries with $M_{\rm tot} \gtrsim 10^8 M_\odot$ occurring at $z \lesssim 1$. This is because the distance from the earth to SMBHs at low redshift is shorter and the mass of SMBHs at low redshift is larger. On the other hand, burst signals with small amplitude ($h_{\rm burst} \lesssim 10^{-17}$) corresponds to coalescence events of "less massive" SMBH binaries with $M_{\rm tot} \lesssim 10^7 M_\odot$ occurring at $z \gtrsim 2$. These events dominate the expected burst event rate provided that the sensitivity of the detector is sufficiently good. This feature is quite important because it breaks the degeneracy be-

tween mass and distance.

Figure 5 shows that the expected region for signal of gravitational wave bursts and the instrumental noise threshold for *LISA*, $h_{\rm inst}$. We compute $h_{\rm inst}$ from the fitting formula for the spectral instrumental noise density of *LISA* [13]. The expected region for $\nu_{\rm burst}[\log(h_{\rm burst}), \log(f_{\rm c})] > 1$ yr^{-1} is above this instrumental noise threshold. For comparison, we show the region for $\nu_{\rm burst}[\log(h_{\rm burst}), \log(f_{\rm c})] > 1/5$ yr^{-1} and $\nu_{\rm burst}[\log(h_{\rm burst}), \log(f_{\rm c})] > 3$ yr^{-1} in figure 5 (b).

From figure 4 and 5, we conclude that the *LISA* can detect intense bursts of gravitational waves at a rate of $\sim 1.0{\rm yr}^{-1}$ assuming that dominant part of these burst events occur at $z \gtrsim 2$. Even in the case of $\epsilon = 0.001$, the *LISA* can detect intense bursts of gravitational waves in one year observation, since $h_{\rm burst} \propto \epsilon^{1/2}$. In addition, we find that large amplitude $h_{\rm burst} \sim 10^{-15}$ signals correspond to coalescence events of massive SMBH binaries $M_{\rm tot} \sim 10^8 M_\odot$ at low redshift $z \lesssim 1$ and small amplitude $h_{\rm burst} \sim 10^{-17}$ signals correspond to less massive SMBH binaries $M_{\rm tot} \sim 10^6 M_\odot$ at high redshift $z \gtrsim 3$.

4. SUMMARY & CONCLUSIONS

In this study, we have estimated the coalescence rate of SMBH binaries in the centers of galaxies using a new SA model of galaxy and quasar formation [4]. Then, we calculated the spectrum of the gravitational wave background from inspiraling SMBH binaries and estimated the expected amplitudes and event rates of intense bursts of gravitational waves from coalescing SMBH binaries [6].

Our SA model includes dynamical friction and random collision as galaxy merging mechanisms, and assumes that a SMBH is fueled by accretion of cold gas during a major merger of galaxies leading to a spheroid formation, and that SMBHs coalesce simultaneously when host galaxies merge. Many previous other studies have paid attention to only SMBH growth and did not take galaxy formation processes into account. For investigating the relations between SMBH growth and galaxy formation processes, SA methods of galaxy and SMBH formation are suitable tools [e.g. 4, 14].

We have found that the gravitational wave background radiation spectrum for $f \lesssim 1\mu$Hz has a characteristic strain $h_c(f) \sim 10^{-16}(f/1\mu{\rm Hz})^{-2/3}$ just below the detection limit from the current measurements of the pulsar timing. The slope of the spectrum for $f \gtrsim 1\mu$Hz gets steep owing to the upper limit in frequency set by the radius of the ISCO. The stochastic background radiation mainly comes from inspiraling SMBH binaries at $0 < z < 1$. Therefore, the background radiation can probe inspiraling SMBH binaries at low redshift.

We have also found that *LISA* might detect intense bursts of gravitational waves owing to the SMBH coalescence events at a rate $0.1 \sim 1.0$ yr^{-1} and that the main contribution to the event rate comes from SMBH binary coalescence events at high redshift $z \gtrsim 2$. Our model predicts that burst signals with a large amplitude correspond to coalescence of large mass SMBH binaries at low redshift while those with a small amplitude correspond to coalescence of small mass SMBH binaries at high redshift. This prediction can be tested by future measurements of the amplitude and the phase evolution in gravitational waves from inspiraling SMBH binaries [13]. Comparing these predictions with observations in future, we can put a stringent constraint on SMBH formation and evolution models.

Acknowledgments

We thank K.S. Thorne and S. Hughes for useful information. MN acknowledges Research Fellowships of the Japan Society for the Promotion of Science for Young Scientists (No.00207). NS is supported by Japanese Grant-in-Aid for Science Research Fund of the Ministry of Education, No.14340290.

References

[1] Haehnelt, M. G., 1994, MNRAS, 269, 199
[2] Jaffe, A. H. & Backer, D. C., 2003, ApJ, 583, 616
[3] Thorne, K. S. & Braginsky, V. B., 1976, ApJ, 204, L1
[4] Enoki, M., Nagashima, M. & Gouda, N. , 2003, PASJ, 55, 133
[5] Nagashima, M., Totani, T., Gouda, N., & Yoshii, Y. 2001, ApJ, 557, 505
[6] Enoki, M., Inoue, K. T., Nagashima, M. & Sugiyama, N. , 2004, ApJ, 615, 19
[7] Binney, J., & Tremaine, S. 1987, Galactic Dynamics, Princeton, NJ, Princeton Univ. Press
[8] Makino, J., & Hut, P. 1997, ApJ, 481, 83
[9] Magorrian, J., et al., 1998, AJ, 115, 2285
[10] Salucci, P., Szuszkiewicz, E., Monaco, P., & Danese, L. 1999, MNRAS, 307, 637
[11] Sesana, A., Haardt, F., Madau, P., & Volonteri, M. 2004, ApJ, 611, 623
[12] Lommen, A. N. 2002, in the Proceedings of the 270. WE-Heraeus Seminar on Neutron Stars, Pulsars and Supernova Remnants, 2002, Physikzentrum Bad Honnef, eds. W. Becker, H. Lesch & J. Truemper.
[13] Hughes, S. A. 2002, MNRAS, 331, 805
[14] Kauffmann, G., & Haehnelt, M. G. 2000, MNRAS, 311, 576